J. F. Rabolt
R. Santo
N. E. Schlotter
J. D. Swalen

Integrated Optics and Raman Scattering: Molecular Orientation in Thin Polymer Films and Langmuir-Blodgett Monolayers

Studies of submicron films and molecular monolayers with infrared and Raman spectroscopy have been hampered by the inability of current spectroscopic techniques to detect the minute amount of material present in these thin-film assemblies. A method for overcoming this problem by using integrated optics has been successfully demonstrated. In the case of Raman studies, the material whose spectrum was desired was made into an asymmetric slab waveguide or a composite waveguide structure in which both the optical field intensity of the in-coupled laser source and the scattering volume of the sample have been significantly increased. Using this technique we have obtained Raman spectra of thin polymer films (<80 nm) and the resonant Raman spectra of single dye monolayers (2.7 nm). Estimates of molecular orientation within the two-dimensional films have been made based on the results of polarized Raman measurements. In addition, the results of overcoating experiments illustrate the versatility and applicability of this technique to a wide variety of surface and thin-film studies.

Introduction

Integrated optical devices have been the subject of many investigations [1, 2] over the past decade primarily motivated by the desire to achieve a compact efficient optical system for the transferral of information. During the development process much has been learned about the fabrication of thin-film waveguides, prism and grating couplers, and other miniature optical components. It was only a matter of time before interest was generated in many other scientific areas [3, 4] where a number of applications of integrated optics awaited.

Only recently have the initial applications of integrated optical techniques used to determine the optical constants [5–7] of polymeric materials appeared in the literature. In these studies the refractive index, absorption, and film thickness were determined by making the material of interest into an asymmetric slab waveguide. Coupling of laser light into the thin films was accomplished using high-index glass prisms, and measurements of the input coupling angles were made for a number of modes of the waveguide structure. Using this information and Maxwell's equations, optical constants were then determined. An extension of these studies into the light-scattering properties (inelastic and quasi-elastic) of thin films [8, 9] has shown considerable promise both as a tool for investigating surfaces and as a means of characterizing the molecular structure of submicron films and Langmuir-Blodgett monolayers.

Raman spectroscopy in particular is a useful characterization tool because of its nondestructive nature. This is of prime importance in polymers which have four levels of structure determining all their important physical properties. In addition to chemical, conformational, and crystal structure, the important morphological features which are dependent upon previous thermal and mechanical history must be characterized in order to fully understand the nature of structure/property relationships. It is therefore imperative that nondestructive spectroscopic techniques be used to probe morphological structure, since they do not alter it in the investigation process.

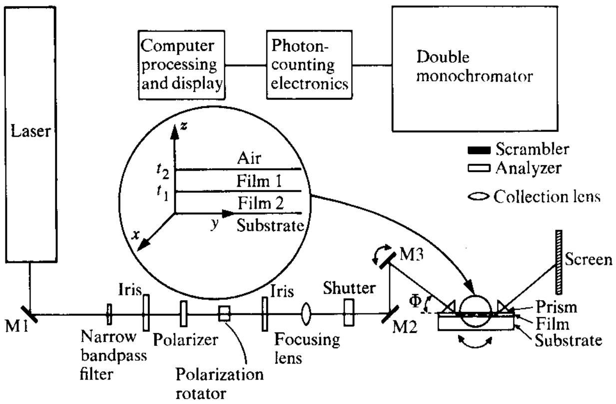

Figure 1 Schematic diagram of apparatus used for Raman scattering experiments.

The application of integrated optical techniques to the study of Raman scattering from thin polymer films and adsorbed molecular monolayers has yielded valuable information concerning molecular orientation and has provided an insight into the nature of intermolecular adhesive forces [8]. The purpose of this work is to outline the experimental techniques used to obtain Raman spectra from submicron films and to describe the results of recent studies on molecular orientation in thin films. This two-dimensional orientation has been determined by varying the input laser polarization and the position and direction of an analyzer placed in the scattered beam. Additional results from overcoating experiments are discussed and illustrated theoretically in order to establish the general applicability of this technique.

Theory

The development of the eigenvalue equation for a three-layered (pyrex substrate, thin film, air) asymmetric slab waveguide has been treated in detail [5]. Mode propagation in the thin-film layer occurs provided that the thickness does not drop below the critical value (≈ 1 μm). To explore submicron films, the composite (four-layer) waveguide structure shown in Fig. 1 was used. Solving Maxwell's equations subject to the appropriate boundary conditions leads to the eigenvalue equation for a four-layered waveguide with the two central layers (Films 1 and 2) both conductive;

$$k_2 t_2 - \arctan (K_3'/K_2) - \arctan (K_1/K_2) = m\pi, \tag{1}$$

where $m = 0, 1, 2, \cdots$, and

$$K_i = \begin{Bmatrix} k_i = (2\pi/\lambda)\,|\,n_i^2 - n_{\text{eff}}^2\,|^{1/2} & \text{for TE} \\ k_i/\varepsilon_i & \text{for TM} \end{Bmatrix},$$

with

$$K_3' = K_3\left[\frac{(K_4/K_3) - \tan k_3 t_3}{1 + (K_4/K_3)\tan k_3 t_3}\right].$$

In this expression n_{eff} is the effective refractive index for each mode and depends on the coupling angle Φ and the refractive index of the coupling prism. TE and TM stand for transverse electrical polarization and transverse magnetic polarization modes. Equation (1) illustrates the parametric dependence on the film thickness of the guiding layers and on the refractive indices n_i of the four components of the asymmetric slab waveguide. Expressions for the electric field $\bar{E}$ in each of the four regions can be derived and provide an insight into light conduction in this type of waveguide structure:

$$\begin{aligned} E_1 &= AC_2C_3 \exp\left[-k_1(z - t_2 - t_3)\right], \\ E_2 &= AC_3[\cos k_2(z - t_3) + (K_3'/K_2)\sin k_2(z - t_3)], \\ E_3 &= A[\cos k_3 z + (K_4/K_3)\sin k_3 z], \\ E_4 &= A\exp(k_4 z), \end{aligned} \tag{2}$$

where

$$\begin{aligned} C_2 &= \cos k_2 t_2 + (K_3'/K_2)\sin k_2 t_2, \\ C_3 &= \cos k_3 t_3 + (K_4/K_3)\sin k_3 t_3, \\ A &= \text{constant}. \end{aligned}$$

In this specific case, traveling waves propagate in Films 1 and 2 while the field is evanescent in both the substrate and superstrate.

In the event that Film 1 (Fig. 1) is below cutoff (due to its refractive index) while Film 2 is conducting, K_3' in Eq. (1) becomes

$$K_3' = K_3\left[\frac{(K_4/K_3) + \tanh k_3 t_3}{1 + (K_4/K_3)\tanh k_3 t_3}\right], \tag{3}$$

and the electric field in Film 1 subsequently becomes evanescent.

Examples in which guided and/or evanescent waves are propagated in Films 1 and 2 due to their choice of refractive index are illustrated in a later section, where they are correlated with the corresponding Raman spectra.

Experimental section

The apparatus used to record the polarized Raman spectra of thin films is schematically illustrated in Fig. 1. In addition to the optics required to select the polarization of the input beam and analyze the scattered light, two rotary stages are required to adjust the coupling angle Φ to the desired value (previously determined from the associated optical constants) so that mode propagation results. Both the mirror M3 and the sample can be rotated about their axes so that the various modes (m values) of the asymmetric waveguide can be selected.

As shown in Fig. 1, the incident laser beam is coupled to the guide using high-index glass prisms (Schott LaSF5) in order to make a large range of $\bar{k}$ vectors available for coupling. The prism is clamped against the film by adjustable thumbscrews (seen in Fig. 2) and an evanescent field traverses the coupling air gap (50–80 nm) and couples the light to the thin film. When a particular Φ value is chosen corresponding to a solution of the eigenvalue equation for a composite asymmetric slab waveguide, the beam propagates inside the film. Raman scattering results from the interaction of the propagating light with the molecules of which the waveguide is composed. Because the beam waist of 150 μm produced by the focusing lens (focal length = 350 mm) is further constrained (in one dimension) to propagate in a slab 1–2 μm thick after coupling, the optical field intensity (OFI) within the film is very high, allowing one to obtain high signal-to-noise (S/N) Raman spectra.

The polarization rotator in Fig. 1 allows the selection of either the TE or TM modes. In TE polarization the electric field vector of the incident laser is parallel to the film surface and perpendicular to the plane of incidence, while in the TM configuration the magnetic field vector of the incident laser is parallel to the film surface and perpendicular to the plane of incidence. Use of both TE and TM polarization in conjunction with an analyzer in the scattered beam allows symmetry assignment of the observed Raman bands and can provide information concerning molecular orientation.

The deposition of polymer films and Langmuir-Blodgett monolayers has been described in detail in an earlier study [5]. An overcoating technique was used to deposit a dye monolayer on water-soluble atactic poly(vinyl alcohol) (PVA) [10]. First, one monolayer of cadmium arachidate was deposited on a pyrex slide such that the hydrocarbon tails projected from the slide. An inverted monolayer of cyanine dye was then deposited, with the chromophore being farthest from the slide. A PVA waveguide was then spin-coated on this assembly and was thus in intimate contact with the dye chromophore.

All Raman spectra were recorded using a Spectra-Physics 165-08 Ar ion laser. The streak produced within the thin film was focused onto the horizontal entrance slit of a Jobin-Yvon Ramanor HG-2S double monochromator interfaced to a Nicolet 1180 for data collection and processing.

Results and discussion

• *Thin polymer films*

Obtaining Raman spectra from 1–2-μm films by making the material of interest into an asymmetric slab waveguide has been described in detail [8]. The advantage afforded by this technique over conventional Raman scattering geometries is particularly important in polymeric materials which form transparent thin films but which are opaque in powder or bulk samples, consequently providing only a limited depth of penetration. In addition, Raman polarization measurements are limited to samples exhibiting good optical properties, since polarization scrambling results when the sample contains crystallites, domains, or voids which are comparable in size to the wavelength of laser excitation. This can lead to confusion over the exact interpretation of the results in terms of depolarization ratios and assignments of band symmetry.

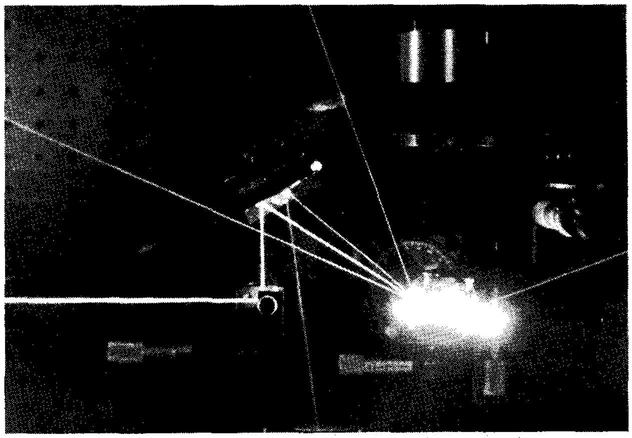

Figure 2 Top view of sampling arrangement for recording Raman spectrum. Laser beam is incident from left. Lens at top right of photograph is used to collect scattered light.

Isotactic poly(methyl methacrylate) (i-PMMA) is an interesting material which was initially thought to exhibit a 5/1 helical chain conformation [11] in the crystalline state. More recently, a re-examination of the x-ray intensity data, together with intermolecular packing calculations, has suggested [12] that the true structure consists of a double-stranded helix containing two chains with the same helical sense and direction. Similar information concerning the molecular structure can be obtained through polarized Raman measurements on thin transparent films. The combination of input polarization and direction of the analyzer in the scattered beam is illustrated in Fig. 3. In the TE mode of the thin-film waveguide two possible directions of the analyzer are possible. If the sample is unoriented, these two measurements, shown in Figs. 4(a–d), determine the depolarization ratio ρ of each vibrational band, which in turn allows assignment to a particular symmetry species [13].

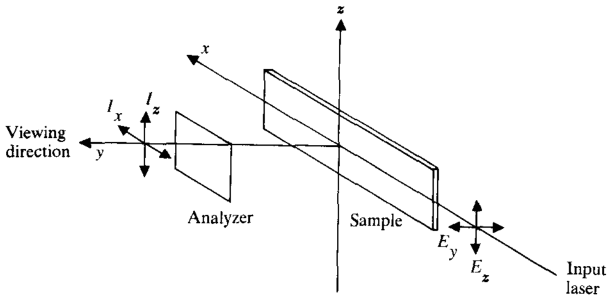

Figure 3 Schematic of input laser polarizations and analyzer positions used for orientation measurements.

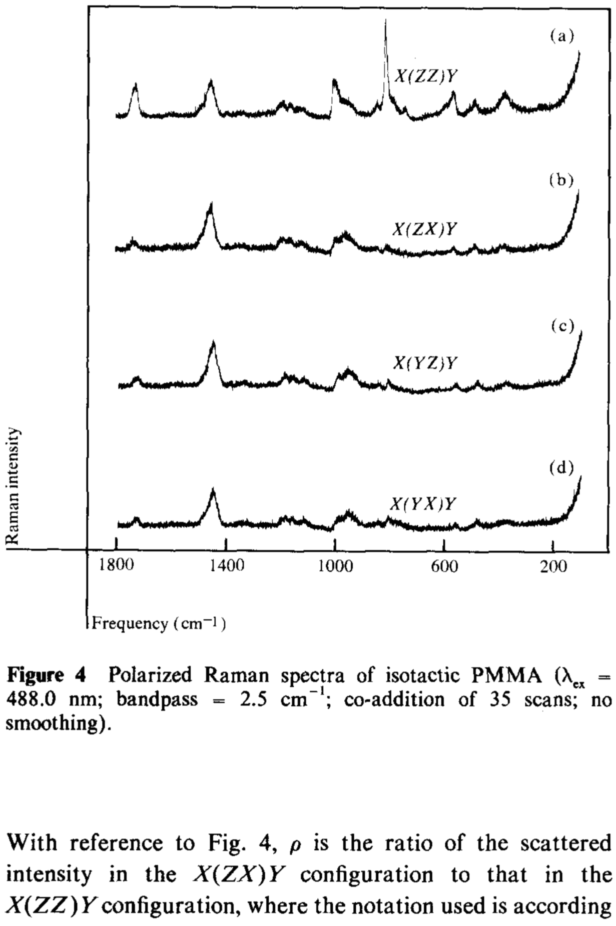

Figure 4 Polarized Raman spectra of isotactic PMMA (λ_{ex} = 488.0 nm; bandpass = 2.5 cm^{-1}; co-addition of 35 scans; no smoothing).

With reference to Fig. 4, ρ is the ratio of the scattered intensity in the $X(ZX)Y$ configuration to that in the $X(ZZ)Y$ configuration, where the notation used is according to Porto [14]. That is, the symbols outside the parentheses are the directions of the incident (left) and scattered (right) radiation, whereas those inside the parentheses refer to the polarization directions of the incident (left) and scattered (right) light. Bands with $\rho < 0.75$ are polarized, while those with $\rho = 0.75$ are depolarized [15]. As can be seen by comparing spectra (a) and (b) in Fig. 4, the bands at 810 and 1730 cm^{-1} that are assigned to motions of the side chain are highly polarized, while that at 1450 cm^{-1} appears to exhibit anomalous polarization. This spectral information in conjunction with a group theoretical analysis based on proposed structural models can be used to identify the correct molecular conformation, and a detailed investigation is in progress.

Additional information concerning the two-dimensional orientation of a polymer film on a substrate can be obtained by considering the resulting Raman spectra when the incident polarization is chosen so that coupling into the TM mode of the waveguide occurs. In a completely isotropic film the spectra obtained using TM excitation with the direction of the analyzer either parallel [$X(YX)Y$] or perpendicular [$X(YZ)Y$] to the scattering plane should be identical. This is illustrated in Figs. 4(c) and (d) for an unoriented i-PMMA film. In the case of a uniaxially or biaxially oriented film, significant relative intensity differences in these two spectral measurements would appear.

- *Multilayered thin-film assemblies*

Waveguide structures composed of two polymer films supported on a substrate were explored as model systems, since several possible applications involve the overcoating of an existing thin film with a polymer overlayer. Additional information concerning the ability to probe various depths of the thin-film assembly by using different modes of the composite waveguide so as to adjust the optical field intensity maxima at various locations within these two films can be obtained through theoretical considerations. The structure of this waveguide is illustrated schematically in Fig. 1, where the general case of two films is shown. The eigenvalue equation which has been derived in an earlier section for this four-layer composite structure contains the parametric dependencies on the optical constants of each of these materials. By choosing various values for the refractive indices (n_1 and n_2) of Films 1 and 2, the optical field intensity which is proportional to $|E|^2$ can be determined in each layer subject to the previously described boundary conditions.

In Fig. 5 a simple case is shown where an atactic poly(methyl methacrylate) (PMMA) block was overcoated with PVA. As can be seen by conducting the laser beam in the PVA layer, the optical field intensity in the PMMA can be changed by choosing different modes (*i.e.*, coupling angles) of the asymmetric slab waveguide. Hence, in this particular experiment the Raman spectrum of the PMMA block was desired and therefore the $m = 1$ mode was selected. PVA was chosen as the overcoating layer because it is a very poor Raman scatterer and is water-soluble, making it easy to wash off the block. Thus, the experiment is nondestructive to the material whose spectrum is being obtained. The Raman spectra obtained from the TE configuration for both the $m = 0$ and $m = 1$ modes of the waveguide are shown in Figs. 6(b) and (c). For comparison, the spectra of the PVA and PMMA homopolymer appear in Figs. 6(a) and (d), respec-

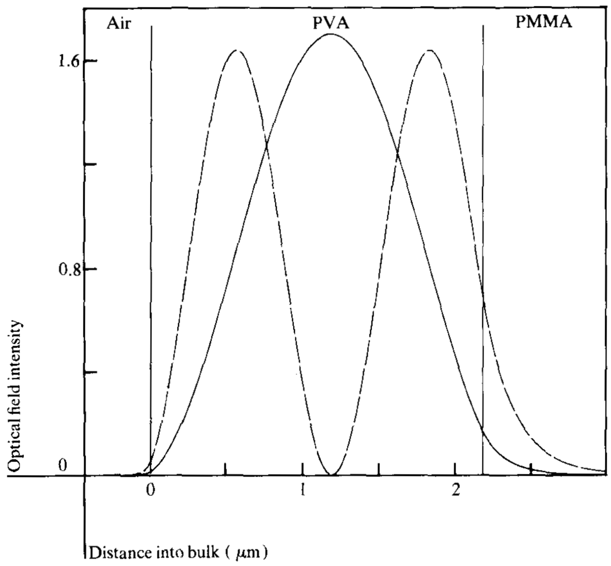

Figure 5 Plot of optical field intensity *vs*. thickness for PVA film on PMMA substrate for $m = 0$ (—) and $m = 1$ (----); $n_{PVA} = 1.5224$, $n_{PMMA} = 1.4945$.

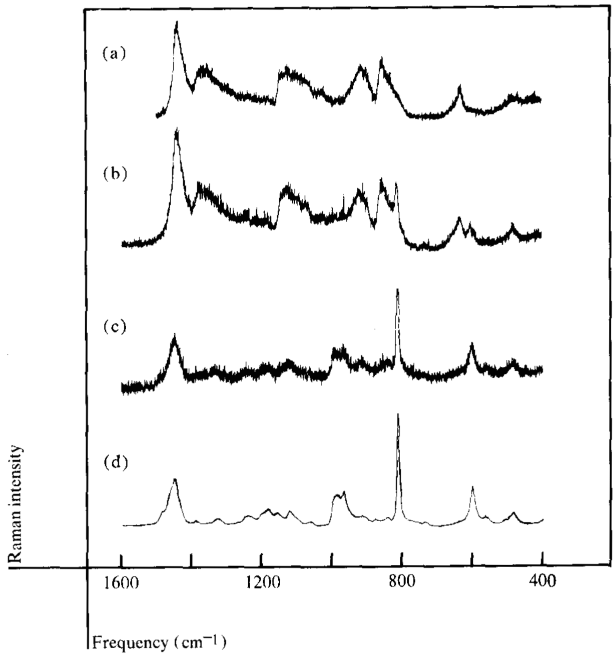

Figure 6 Raman spectra of bulk PVA (a), PVA/PMMA waveguides with $m = 0$ (b) or $m = 1$ (c), and bulk atactic PMMA (d) ($\lambda_{ex} = 488.0$ nm; bandpass = 4 cm^{-1}; no smoothing).

tively. What becomes immediately apparent is that as the optical field intensity is increased within the PMMA block for the $m = 1$ mode, its Raman spectrum dominates because it has a significantly larger scattering cross section than that of PVA. Comparison of Figs. 6(c) and (d) indicates that very little residual intensity of the PVA bands remains. The importance of this illustrative example lies in the fact that the structure of the substrate (in this case, PMMA) could be explored nondestructively by this simple overcoating technique.

Further examples of the versatility of the overcoating technique are shown for a PVA overcoat on PMMA [Fig. 7(a)] with $n_{PVA} > n_{PMMA}$ and for a PVA overcoat on PS [Fig. 7(b)] with $n_{PVA} < n_{PS}$. In the former example, the optical field intensity (OFI) for the $m = 0$ and 1 modes is larger in the PVA layer, with a residual evanescent or conducting field extending within the PMMA. It is interesting to note that when choosing the $m = 1$ mode, there is a maximum in the OFI at the interface between the PVA and PMMA films; hence, it would be possible to investigate Raman scattering from this point within the film. On the other hand, the $m = 2$ mode has a high OFI within the PMMA, with a considerably reduced field inside the PVA. Since PVA has a much smaller Raman scattering cross section, the spectrum of the composite film will be dominated by bands attributable to PMMA. Therefore, by selecting the appropriate mode of the asymmetric slab waveguide, it is possible to probe various regions of the composite film.

Another informative example, in which polystyrene (PS) is overcoated with PVA, is depicted in Fig. 7(b). By comparison, the mode pattern is considerably different from that of the previous example and reflects the fact that $n_{PS} > n_{PVA}$. In contrast, the OFI corresponding to $m = 0$ is a maximum in the PS, whereas the modes with higher m values have an OFI distribution throughout both the PS and PVA films. Again, the Raman spectrum from the $m = 0$ mode would be dominated by PS since it is a very strong Raman scatterer. Coupling of the laser light into waveguide modes of higher m values would increase the OFI in the PVA, and the observed Raman spectrum would contain contributions from both PVA and PS.

In general, it should be pointed out that the beauty of the overcoating process is that it is very versatile in allowing not only the nondestructive evaluation of polymer films but also the probing of films at various depths by simple mode selection of the asymmetric slab waveguide.

Langmuir-Blodgett dye monolayers

Studies [8] have shown that the resonant Raman spectrum of a single cyanine dye monolayer (see Structure I)

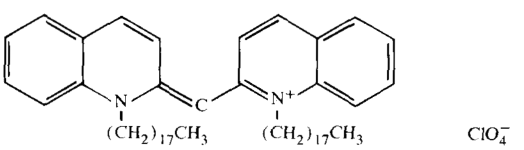

(I)

1,1′-Dioctadecyl-2,2′-cyanine perchlorate

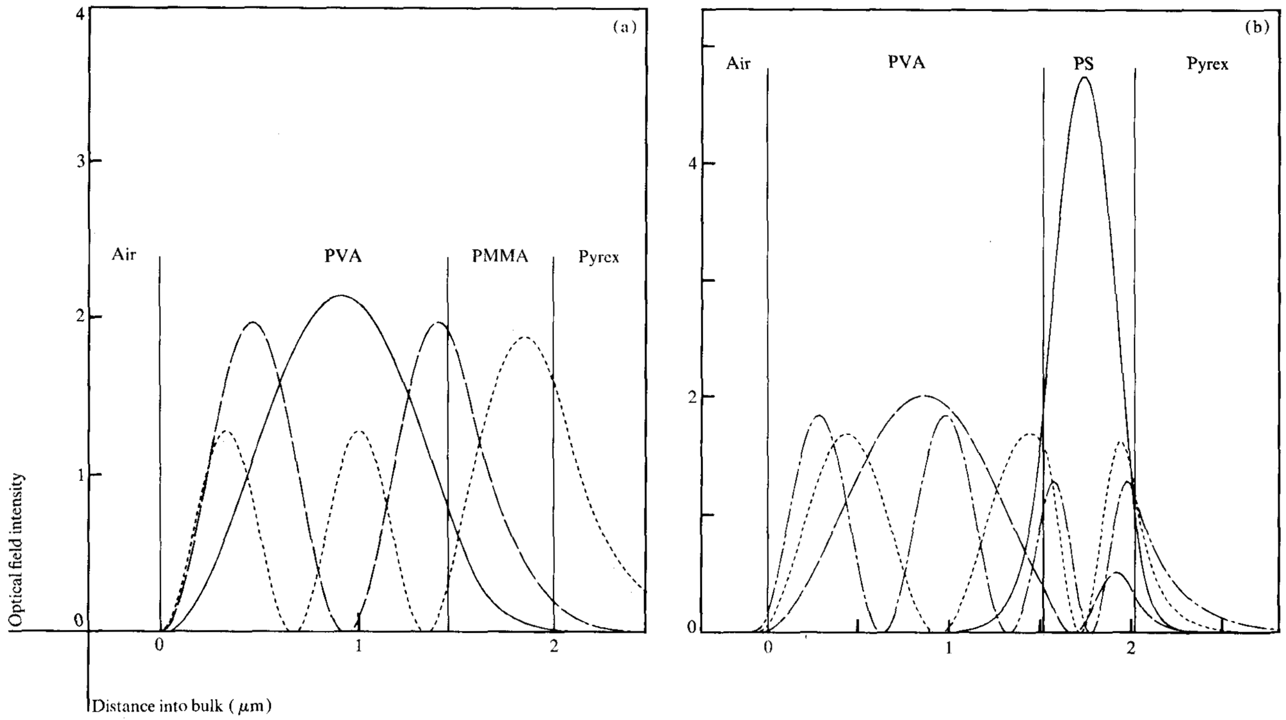

Figure 7 Plots of optical field intensity *vs.* thickness for (a) PVA/PMMA and (b) PVA/PS composite waveguides for $m = 0$ (—), 1 (— —), 2 (---), and 3 (— · —); $n_{PVA} = 1.5224$, $n_{PMMA} = 1.4945$, and $n_{Pyrex} = 1.4706$.

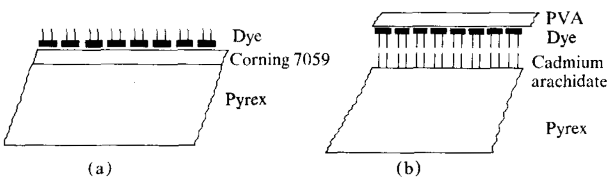

Figure 8 (a) Dye monolayer (see Structure I) deposited on Corning 7059 glass; (b) sample configuration for investigating PVA/dye interaction.

deposited on a Corning 7059 glass waveguide, as illustrated in Fig. 8, could be obtained because of the high OFI generated within the guiding layer. Upon comparison with a spectrum obtained from bulk cyanine crystals, it was discovered that a number of bands had undergone both frequency shifts and intensity changes, especially in the 1300–1450-cm^{-1} region. This was attributed to the perturbation of several modes of the quinoline chromophore, assigned to ring C-C and C-N stretching vibrations, by the surface groups of the Corning glass. To further elucidate this adhesive interaction, cyanine dye monolayers were deposited on PVA in the configuration shown. It was expected that the strong polar hydroxyl groups would increase the intermolecular interaction with the cyanine dye chromophore by the formation of hydrogen bonds with the nitrogen atom of the quinoline ring. The resulting spectrum is shown in Fig. 9, where it is compared with those obtained for bulk crystals and a monolayer deposited on Corning glass. In addition to the shift of the 1390- and 1363-cm^{-1} bands to lower frequency, there is a third broad component located at 1374 cm^{-1}. This component is not present in a solid solution of Structure I and PVA and thus appears to be related to the interaction and/or orientation of the chromophores on a two-dimensional surface. A recent Raman study [16] of cyanine dye crystals indicates that resonance interaction between the ring-stretching modes of the two quinoline moieties coupled through the conjugated bridge can explain the presence of a doublet at 1361 and 1380 cm^{-1} due to in-phase and out-of-phase coupling. Any distortion in the chromophore geometry due to the constraints imposed by deposition on a two-dimensional surface and strong intermolecular hydrogen bonding with the surface would conceivably perturb that coupling, giving rise to a distribution of in-phase and out-of-phase ring-stretching modes similar to what is actually observed. The observed frequencies of the stronger bands in the three spectra of Fig. 9 are listed in Table 1, together with their assignments.

The question of chromophore orientation on the PVA surface was also addressed through polarized resonance Raman scattering. Although the polarizability tensor may

Table 1 Observed Raman bands in Structure I (λ_{ex} = 476.5 nm).

Bulk crystals	*Monolayer on Corning 7059*	*Monolayer on PVA*	*Assignment*
1632	1632	1631	exo C=C str
1392	1390	1386	C—C str + C—N str
—	—	1374	
1366	1363	1359	C—C str + C—N str + CH ipb

str – stretching, ipb – in-plane bending.

become asymmetric near resonance, resulting in observance of anomalous polarizations, it is possible to get a qualitative indication of molecular orientation if the direction of the electronic transition moment of the chromophore is known. In Structure I the transition moment responsible for absorption throughout the visible was shown to be parallel to the long axis of the cyanine chromophore. This fact can be used in conjunction with resonance Raman measurements to eliminate one of the three possible chromophore orientations on the PVA surface. Coupling of the incident polarized light into the TE mode gives rise to resonance Raman scattering [see Fig. 10(a)] if the chromophores are situated on the surface such that the incident electric field vector couples with the electronic transition moment. This is the mechanism responsible for selective enhancement of the scattering cross section of the chromophore by four to six orders of magnitude, and would occur if the plane of the chromophore were parallel to the surface or the chromophore was on its edge so that its transition moment was still parallel to that surface. On the other hand, if the polarization of the incident electric field is rotated by 90° to couple into the TM mode of the waveguide, interaction with the electronic transition can only occur if the long axis of the chromophore is oriented perpendicular to the PVA surface. The resulting spectra obtained in these two cases are shown in Fig. 10(b). Resonance Raman scattering occurs predominantly in the TE configuration, giving rise to the expected spectrum in the 1300–1400-cm^{-1} region. In contrast, with TM polarization the spectrum is dramatically reduced, indicating that the chromophores do not have their transition moments perpendicular to the surface. The small amount of residual intensity of the 1390-cm^{-1} band in the TM spectrum can be adequately explained by surface roughness ("hills and valleys" would cause the transition moment of the chromophore not to be truly perpendicular to the direction of the TM electric field component) and light propagation in a waveguide which is not parallel to the surface but inclined at some small angle [8]. In a TM mode there is a small component of the electric field parallel to the surface which can subsequently couple with the transition moment of the chromophore; hence, some residual intensity persists. These

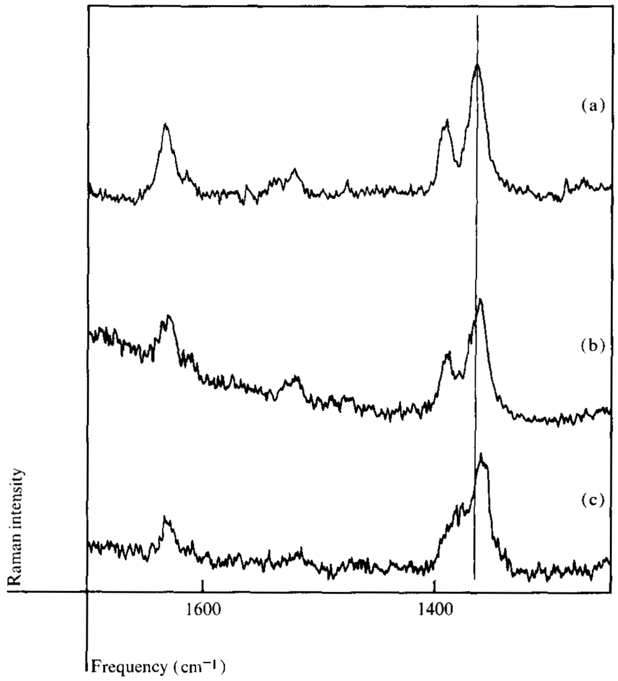

Figure 9 Raman spectra of (a) bulk cyanine crystals and monolayers of Structure I deposited on (b) Corning 7059 glass and (c) PVA.

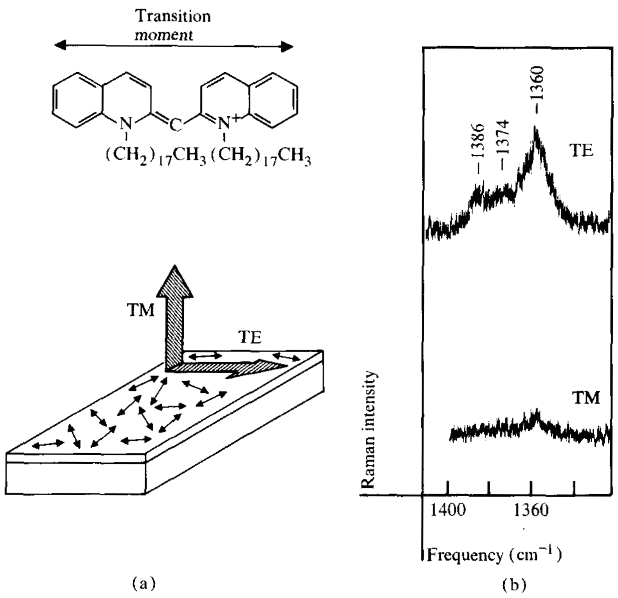

Figure 10 (a) Schematic of chromophore orientation on waveguide surface and input laser polarization for TE and TM modes of propagation. (b) Resonant Raman spectra in the 1320–1420-cm^{-1} region of the spectra obtained for TE and TM modes. No analyzer was used.

results correlate very well with those from visual observations. When coupled into the TE mode, the length of the streak in the dye/PVA film is 1–2 mm (λ = 476.5 nm) due to absorption by the dye caused by coupling between the incident polarization and the transition moment vectors. In the TM configuration the streak in the film traverses the entire distance (25 mm) between the prisms, since little absorption occurs. This is the visual analog of the resonance Raman experiment and supports earlier conclusions [17] regarding chromophore orientation on the PVA surface.

Conclusion

A number of examples have been presented which demonstrate that integrated optical techniques in conjunction with Raman spectroscopy provide for nondestructive evaluation of thin organic films. The ability to study single monolayers (2–3 nm) deposited on solid surfaces has provided useful information concerning the nature of intermolecular adhesive forces and an insight into molecular orientation at the surface. This technique has been shown, in general, to be very versatile and promises to be applicable in a wide range of surface and thin-film studies.

Acknowledgment

We would like to express our gratitude to Y. Y. Cheng and C. Snyder for providing high-quality dye materials for these studies.

References and note

1. P. K. Tien, "Light Waves in Thin Films and Integrated Optics," *Appl. Opt.* **10,** 2395–2413 (1971).
2. D. Marcuse, *Theory of Dielectric Optical Waveguides,* Academic Press, Inc., New York, 1974, Ch. 1–2.
3. Y. Levy, C. Imbert, J. Cipriani, S. Racine, and R. Dupeyrat, "Raman Scattering of Thin Films as a Waveguide," *Opt. Commun.* **11,** 66 (1974).
4. Y. Levy and R. Dupeyrat, "Méthodes d'Etude de Couches Minces et d'Interfaces par Spectroscopie Raman," *J. Phys. Coll.* **C5-38** (Suppl. 11), 253–260 (1977).
5. J. D. Swalen, R. Santo, M. Tacke, and J. Fischer, "Properties of Polymeric Thin Films by Integrated Optical Techniques," *IBM J. Res. Develop.* **21,** 168–175 (1977).
6. J. D. Swalen, M. Tacke, R. Santo, K. E. Rieckoff, and J. Fischer, "Spectra of Organic Molecules in Thin Films," *Helv. Chim. Acta* **61,** 960–977 (1978).
7. J. D. Swalen, "Optical Wave Spectroscopy of Molecules at Surfaces," *J. Phys. Chem.* **83,** 1438–1445 (1979).
8. J. F. Rabolt, R. Santo, and J. D. Swalen, "Raman Spectroscopy of Thin Polymer Films Using Integrated Optical Techniques," *Appl. Spectrosc.* **33,** 549–551 (1979); "Raman Measurements on Thin Polymer Films and Organic Monolayers," *Appl. Spectrosc.* **34,** 517–521 (1980).
9. N. L. Rowell and G. I. Stegeman, "Brillouin Scattering from Surface Phonons in Thin Films," *Phys. Rev. Lett.* **41,** 970–973 (1978).
10. Throughout this paper atactic polymers are abbreviated using the name of the polymer only, whereas isotactic polymers are abbreviated by prefixing the abbreviated polymer name with an i (*e.g.,* PMMA *vs.* i-PMMA).
11. H. Tadokoro, Y. Chatani, H. Kusanagi, and M. Yokoyama, "Structure of Isotactic Poly(methyl methacrylate)," *Macromolecules* **3,** 441–447 (1970).
12. H. Kusanagi, H. Tadokoro, and Y. Chatani, "Double Stranded Helix of Isotactic Poly(methyl methacrylate)," *Macromolecules* **9,** 531–532 (1976).
13. R. G. Snyder, "Raman Scattering Activities for Partially Oriented Molecules," *J. Mol. Spectrosc.* **37,** 353–365 (1971).
14. S. P. S. Porto, "Angular Dependence and Depolarization Ratio of the Raman Effect," *J. Opt. Soc. Amer.* **56,** 1585–1589 (1966).
15. H. W. Siesler and K. Holland-Moritz, *Infrared and Raman Spectroscopy of Polymers,* Marcel Dekker, Inc., New York, 1980, Ch. 4.
16. L. G. Pace and E. L. Pace, "Raman Spectrum of 1,1'-Diethyl-2,2'-cyanine Iodide Near the π-π^* Electronic Transition," *Spectrochimica Acta* **36A,** 557–561 (1980).
17. J. F. Rabolt, N. E. Schlotter, J. D. Swalen, and R. Santo, unpublished results.

Received January 22, 1981; revised September 16, 1981

J. F. Rabolt, N. E. Schlotter, and J. D. Swalen are located at the IBM Research Division laboratory and R. Santo is located at the IBM General Products Division laboratory, both at 5600 Cottle Road, San Jose, California 95193.